Ultrasound in Med. & Biol., Vol. 39, No. 10, pp. 1915–1924, 2013

0301-5629/$ - see front matter

http://dx.doi.org/10.1016/j.ultrasmedbio.2013.04.005

● *Original Contribution*

CREANUIS: A NON-LINEAR RADIOFREQUENCY ULTRASOUND IMAGE SIMULATOR

François Varray,*† Olivier Basset,* Piero Tortoli,† and Christian Cachard*
*CREATIS, Université de Lyon, CNRS UMR 5220, Inserm U1044, Université Lyon 1, INSA-Lyon, Villeurbanne, France; and
†Microelectronics Systems Design Laboratory, Università degli Studi di Firenze, Florence, Italy

(*Received* 24 *September* 2012; *revised* 29 *March* 2013; *in final form* 4 *April* 2013)

Abstract—Nonlinear ultrasound methods are widely used in clinical applications for tissue or contrast harmonic imaging. Accurate non-linear imaging simulation tools are required in research studies for the development of new methods. However, in existing simulators, the possible inhomogeneity of the coefficient of non-linearity, which is generally observed in tissue and in particular when contrast agents are involved, has not yet been implemented. This article describes a new ultrasound simulator, called CREANUIS, devoted to the computation of B-mode images where both linear and non-linear propagation in media is considered, with a possible inhomogeneous coefficient of non-linearity. The resulting fundamental images, based on a spatially variant and non-linear point spread function, are in accordance with those obtained through the reference linear FieldII simulator, with computation time reduced by a factor of at least 1.8. Non-linear images of media exhibiting inhomogeneous coefficients of non-linearity are also provided. The simulation software can be freely downloaded from our website. (E-mail: francois.varray@creatis.univ-lyon1.fr) © **2013 World Federation for Ultrasound in Medicine & Biology.**

Key Words: **Ultrasound non-linearity, Coefficient of non-linearity, Non-linear propagation, Radiofrequency image simulation.**

INTRODUCTION

Non-linear propagation of ultrasound (US) waves in tissue has been used for more than 10 years for harmonic imaging and tissue harmonic imaging (THI). All these methods are aimed at achieving a higher spatial resolution with respect to classic imaging methods. In particular, THI exploits the native generation of harmonics directly associated with non-linear propagation (Averkiou et al. 1997; van Wijk and Thijssen 2002). The harmonics increase is related to the coefficient of non-linearity, which has different values in healthy and pathologic tissues (Zhang and Gong 1999) and particularly high values in ultrasound contrast agents (UCAs) (Wu and Tong 1998). However, when UCAs are injected into blood, another mechanism, besides non-linear propagation, is involved, that is, the acoustic response of the microbubbles themselves. This mechanism has been thoroughly studied by several authors (Bouakaz et al. 1998; de Jong 1993; Mari et al. 2010; Tang and Eckersley 2007) because it can be exploited to improve the contrast-to-tissue ratio in US images. Several techniques have been proposed for this aim, such as pulse inversion (PI) (Simpson et al. 1999), pulse substraction Doppler (Mahue et al. 2011), non-linear Doppler (Didenkulov et al. 1999), power modulation (PM) (Eckersley et al. 2005), second-order ultrasound field (SURF) imaging (Angelsen and Hansen 2007), pulse subtraction time delay (Borsboom et al. 2009), parametric imaging (Rognin et al. 2010), second-harmonic reduction (SHR) (Pasovic et al. 2010) and second-harmonic inversion (SHI) (Pasovic et al. 2011). However, Tang and coworkers (Tang and Eckersley 2006; Tang et al. 2011) have recently reported that in these cases, the non-linear propagation effect cannot be neglected, as it may be at the origin of discrepancies between expected and actual images (Tang and Eckersley 2006; Tang et al. 2011).

Notwithstanding the high interest in non-linear propagation, the correlated simulation tools have limitations that prevent their extensive use in non-linear imaging. For example, the well-known FieldII software (Jensen 1996; Jensen and Nikolov 2000; Jensen and Svendsen 1992) simulates linear propagation as well as beamforming from any US probe. However, FieldII does not simulate non-linear propagation, even though

Address correspondence to: François Varray, 7 Avenue Jean Capelle, 69621 Villeurbanne, France. E-mail: francois.varray@creatis.univ-lyon1.fr

preliminary approaches have been proposed to overcome this limitation (Du and Jensen 2008; Du et al. 2010). On the other hand, non-linear propagation is considered the solution to the Khokhlov-Zabolotskaya-Kuznetsov *(KZK)* and Westervelt equations. These methods are based on finite-difference schemes (Hallaj and Cleveland 1999; Yang and Cleveland 2005), on spectral approaches (Szabo 1978; Christopher and Parker 1991b) or on the split-step method (Christopher and Parker 1991a; Zemp et al. 2003). A major limitation of these approaches is the long computation time, which assumes reasonable values only when the angular spectrum method (ASM) is used to compute the fundamental and second-harmonic components. However, none of the mentioned approaches has specifically investigated the possible inhomogeneity of the coefficient of non-linearity. An exception is represented by the work of Demi et al. (2011), whose iterative non-linear contrast source method allows simulating media with inhomogeneity in terms of both attenuation and coefficient of non-linearity. However, the computation time is here too large and limits its use in image simulation. This problem is overcome with the generalized angular spectrum method (GASM), which quickly computes the 4-D (3-D + t) evolution of the fundamental and second-harmonic components for any 2-D sources with possible inhomogeneity of the coefficient of non-linearity (Varray et al. 2011b). The method, suitable for implementation on a graphic processor unit (GPU), computes the total pressure field in a couple of seconds (Varray et al. 2011a).

The simulation of non-linear radiofrequency (RF) images has been discussed in a few papers. Li and Zagzebski (2000) used a finite-difference scheme to compute the non-linear field and a time delay algorithm to create the image. To simplify the non-linear field computation, only a piston source was considered. Pinton et al. (2009) proposed a complete 3-D finite difference model to simulate the non-linear propagation of an US wave for a linear array and a time delay algorithm to create the US image. However, by use of a cluster of 56 processors with 112 GB of memory, one image was obtained in 32 h. This method is thus currently not usable for intensive simulation. Yu et al. (2011) simplified the propagation equation to reduce the total computation time by considering only the two dominant effects for harmonic imaging: non-linearity and relaxation attenuation. Treeby et al. (2011) used the full wave equation, a k-space pseudo-spectral method and, to more quickly compute harmonic images, a performing GPU. None of the simulation tools considered the spatial impulse response of the transducer, thus limiting the acoustical performance and the realism of the simulation, nor the possible medium inhomogeneity in terms of the coefficient of non-linearity.

In this article, a novel tool, CREANUIS (Nonlinear Ultrasound Image Simulation software developed at the CREATIS laboratory), is proposed to simulate RF images containing the fundamental and second-harmonic components generated by the US wave in media with either homogeneous or inhomogeneous non-linear behavior. CREANUIS has been designed to combine the information of a non-linear US field with an arbitrary scatterers' distribution. Because the reflected energy and, consequently, the non-linear effect are very low during back-propagation, the fundamental and harmonic components of back-scattered echoes are computed considering only the forward path.

The article is organized as follows. First, the software is described and the hypotheses made for the image construction are highlighted. Then, sample images obtained with CREANUIS are presented. The fundamental images are compared with the corresponding FieldII images. The simulated second-harmonic images and some additional features of CREANUIS, such as the reduced computation time, are presented. Finally, the main benefits and drawbacks of the proposed software are discussed.

SOFTWARE DESCRIPTION

CREANUIS generates US images by repeating the same basic operations for each simulated line. For a given probe geometry, CREANUIS first uses GASM to compute the non-linear US field at fundamental and second-harmonic frequencies. Then, the non-linear RF echo signals are calculated considering the fundamental and second-harmonic components of the pressure impinging on each scatterer, by taking into account the spatially variant point spread function (PSF) and the coefficient of non-linearity.

To run the simulator, first information on the global geometry of the probe, the scatterers' distribution (positions and amplitudes) and the medium's coefficient of non-linearity map must be given. Second, the active part of the probe has to be selected to compute the 4-D (3-D + t) field for the first and second harmonic components. Then the back-scattering echoes are computed as a function of the scatterers' position and the chosen beamforming strategy. One line of the B-mode image is finally obtained. The procedure is repeated for the adjacent lines by dynamically selecting new sets of active transducer elements. The receive beamforming scheme is illustrated in Figure 1.

Nonlinear ultrasound field

Non-linear propagation was simulated through the GASM (Varray et al. 2011b). The GASM quickly provides the pressure field for the selected 3-D media.

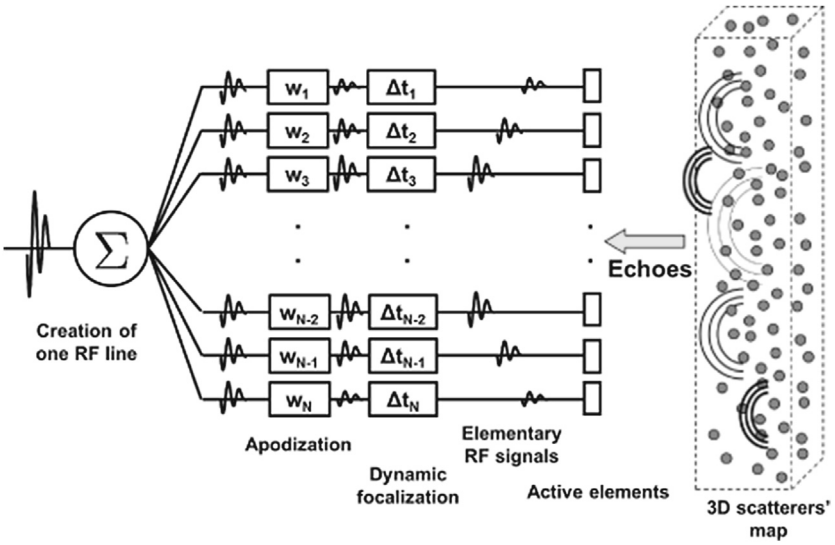

Fig. 1. Illustration of the receiver beamforming strategy to produce one radiofrequency (RF) line. The w_i coefficients are the weighting coefficients of the apodization on the ith element, and the Δt_i coefficients are the time delays used in the dynamic focalization on the ith elementary radiofrequency line.

The transmission beamforming strategy (focalization, windowing and apodization) can be easily implemented in the simulation. The fundamental (p_1) and second-harmonic (p_2) pressure wave components are expressed as

$$p_1(x,y,z,t) = \mathcal{F}^{-1}\left(P_0\left(k_x,k_y,z_0,k_t\right)e^{-iK(z-z_0)}\right) \quad (1)$$

$$p_2(x,y,z,t) = \mathcal{F}^{-1}\left(\frac{-ik_t^2}{2K\rho_0 c_0^2}\left(\int_{z_0}^{z}\mathcal{F}\left(\beta(x,y,z)p_1^2(x,y,z,t)e^{iKu}du\right)\right)e^{-iK(z-z_0)}\right) \quad (2)$$

with the different variables defined in Table 1. K is the complex 3-D wavenumber expressed as

$$K\left(k_x,k_y,k_t\right) = \sqrt{k_t^2-k_x^2-k_y^2}-i\alpha(f) \quad (3)$$

where a(f) is the attenuation of the medium. The GASM attenuating model takes into account the frequency-dependent attenuation of the medium, which is defined by

$$\alpha(f) = \alpha_0\left(\frac{f}{1e6}\right)^{\gamma} \quad (4)$$

where f = frequency of the transmitted signal (in Hz); α_0 = attenuation constant of the medium (in $\mathrm{Np\cdot m^{-1}\cdot MHz^{-\gamma}}$); and γ = a number between 1 and 2 for biological media.

Radiofrequency image simulation

Scatterers' distribution. In CREANUIS, the scatterers are considered as a collection of isolated point targets characterized by their 3-D coordinates and their back-scattering amplitudes. The scatterers' map can be randomly set, imported from other simulations such as those based on FieldII (Jensen 1996) or defined by the user. Usually, the back-scattering amplitude is distributed according to a normal distribution with a standard deviation of 1, but different statistics can be used.

Elementary RF signals. The echo signals are simulated through the following operations. For a given scatterer spatial position, the fundamental and second-harmonic contributions are extracted from the computed field. The secondary back-scattered spherical wave is computed, with amplitude depending on the scatterer response. Attenuation is taken into consideration for both the propagation and the back-propagation paths.

Table 1. Variables

x, y, t	Spatial dimension
t	Temporal dimension
z_0	Initial position of the probe
β	Coefficient of non-linearity map
ρ_0	Density
c_0	Speed of sound
$\mathcal{F}$ and $\mathcal{F}^{-1}$	2D+t Fourier transform and inverse Fourier transform in the x, y, and t dimensions
k_x, k_y, k_t	Wavenumber in the x, y and t direction
P_0	Fourier transform of the source wave at the original position z_0

The pressure actually received by the probe depends on the position of the scatterer and on the geometry of the transducer. To take this interaction into account, the spatial impulse response of the transducer is computed according to the formulation proposed by Stepanishen (1971) and adopted by Jensen and Svendsen (1992).

Final RF line. The RF echoes received by each active element are combined according to the desired receiver beamforming strategy to produce one RF line of the image (Fig. 1). Dynamic focalization is implemented, but other strategies could be used. Possible receiver apodization is directly set by the user.

Nonlinear image computation

The previous operations are repeated for each line of the image. The final data contain both the fundamental and second-harmonic information provided by the 4-D pressure field. The two components are mixed together according to the default settings of CREANUIS, but when needed, they can be separated through an appropriate bandpass filter.

Software implementation and utilization

CREANUIS is implemented in C++. The memory needed in the simulation depends, in particular, on the discretization used for the medium. A spatial discretization is required for the pressure field and the 2-D + t matrix used in the Fourier domain. Typical usable values for the (x, y, t) grid range from (64, 64, 256) to (256, 128, 1024). The dimensions of the grid also depend on simulation parameters such as the number of computed lines, number of active elements, sampling frequency, speed of sound (which is assumed constant) and axial depth range.

To save time, the GASM simulation can be disabled if the field has already been simulated. For media with inhomogeneous coefficients of non-linearity, the GASM simulation has to be repeated for each active aperture of the probe during creation of the image.

NUMERICAL PHANTOM, TRANSMISSION PARAMETERS AND QUANTIFICATION METHODS

To evaluate the proposed model, three different simulation cases have been considered. In each case, the main transmission parameters and the medium characteristics are provided.

Case 1. homogeneous medium

The first medium corresponds to a homogeneous tissue ($40 \times 10 \times 40$ mm) made using a random distribution of 600,000 scatterers (30 scatterers/mm^3). A Hanning apodization is set in both transmission and reception on the 64 active elements. Hanning-windowed three-cycle sinusoidal bursts at 5.0 MHz are transmitted in the medium and focused at 40 mm. The same scattering distribution (position and amplitude) has been used in simulations with either FieldII or CREANUIS.

Case 2. cyst phantom

The second simulated object is similar to the cyst phantom defined in Jensen and Munk (1997). It is composed of a homogeneous background including hyper- and hypo-echoic areas of different sizes and points targets. Hanning-windowed three-cycle sinusoidal bursts at 3.5 MHz are here focused at 60 mm. Hanning apodization is set in both transmission and reception.

Case 3. inhomogeneous coefficient of non-linearity

To simulate media with inhomogeneous coefficients of non-linearity, it is necessary to provide the coefficient of non-linearity map of the medium. Each RF line is created using the appropriate volume from the coefficient of non-linearity map of the wave path. In the example presented in the next section, a medium divided into two parts is considered: the right half has a coefficient of non-linearity $\beta = 3.5$, and the left half, $\beta = 7$ (see Fig. 5a). A random distribution of 100,000 scatterers is used (4.5 scatterers/mm^3). The same transmission settings adopted for the cyst phantom (case 2) are used in transmission and reception.

Pulse inversion transmission

To illustrate CREANUIS' suitability to simulate different harmonic imaging techniques, the pulse inversion (PI) technique was selected. A PI image is obtained, first, through a GASM simulation with a transmitted phase of 0°. Then a second simulation with a 180° phase is carried out for the same scatterers' map and backscattering amplitudes. The PI image is obtained by adding together the two simulated RF images.

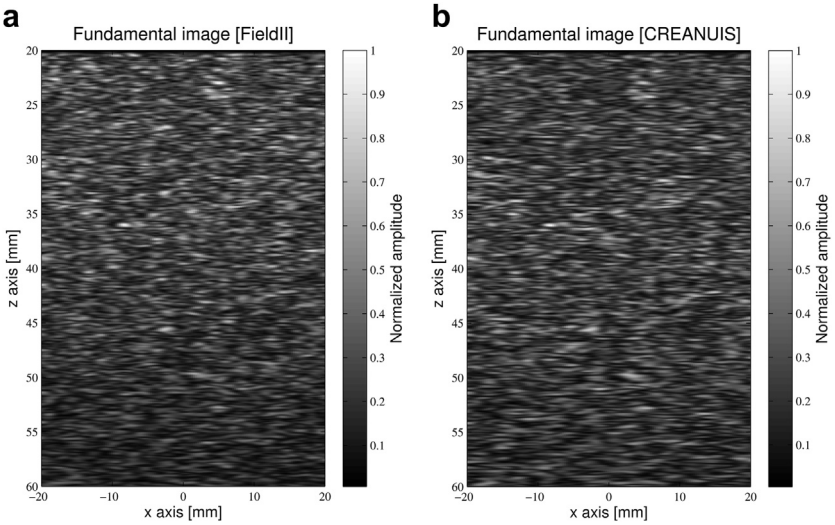

Fig. 2. Fundamental B-mode images of a random scatterer's distribution (30 scatterers/mm^3) obtained with (a) FieldII and (b) CREANUIS.

Quantification

To quantify the difference between the images obtained with FieldII and CREANUIS, a first-order statistical evaluation is conducted. The mean deviation (MD) between the intensities of each pixel in the images simulated by the two models is computed as

$$\mathrm{MD} = \frac{1}{nm} \sum_{1}^{n} \sum_{1}^{m} \left| I_{i,j}^{\mathrm{FieldII}} - I_{i,j}^{\mathrm{CREANUIS}} \right| \qquad (5)$$

where $I_{i,j}^{X}$ = pixel intensity in the X image of dimension (n, m). The speckle distributions of the simulated images are also estimated. For each image, the root mean square error (RMSE) between the theoretical Rayleigh distribution and the actual distribution is then computed (Bernard et al. 2006) as

$$\mathrm{RMSE} = \frac{1}{N} \sum_{i=1}^{N} (R_i - X_i)^2 \qquad (6)$$

where R_i = probability of intensity i in the Rayleigh distribution; X_i = probability of intensity i in the simulated X image; and N = number of bins defined in the statistical distribution.

To estimate the axial and lateral resolution of an ultrasound image, the cross-correlation method proposed by Wagner et al. (1983) was used.

RESULTS

Comparison with FieldII

By use of the medium described in case 1, normalized fundamental B-mode images were obtained using FieldII and CREANUIS (Fig. 2a and 2b, respectively). The means ± standard deviations in the FieldII and CREANUIS images are 0.208 ± 0.123 and 0.211 ± 0.115, respectively. The MD between the two images is 8.1%.

The probability density functions estimated for the two images are compared with the Rayleigh distribution in Figure 3. The RMSEs for the FieldII and the CREANUIS images are 7.7% and 2.1%, respectively.

Novel features of CREANIUS

Second harmonic imaging. For the cyst medium (case 2), the fundamental images obtained with FieldII and CREANUIS are presented in Figure 4a and b, respectively. The second-harmonic image provided by CREANUIS is displayed in Figure 4c. In both fundamental images, the resolution in the axial and lateral directions is 0.32 and 1.91 mm, respectively. In the second harmonic image, the resolution decreased to 0.28 and 1.55 mm. Note that the gray scale (in dB) is different in Figure 4c because of the lower pressure field obtained for the second-harmonic component.

Simulation of a medium with an inhomogeneous coefficient of non-linearity. The simulation of a medium with an inhomogeneous coefficient of non-linearity (case 3) provided the images in Figure 5. In the fundamental image (Fig. 5b), no coefficient of non-linearity variation is visible. However, in the second-harmonic image (Fig. 5c), image intensity differs between the left and right parts: as expected, the larger the coefficient of non-linearity is, the higher is the second-harmonic amplitude.

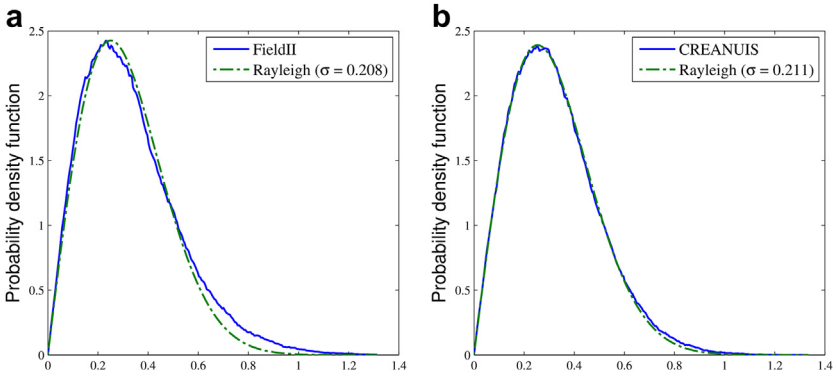

Fig. 3. Theoretical Rayleigh probability density function obtained with (a) FieldII and (b) CREANUIS. The root mean square error obtained with FieldII is 7.7%, and that obtained with CREANUIS, 2.1%.

Nonlinear imaging: pulse inversion example. The cyst phantom and the transmission settings used in case 2 were adopted also for PI simulations. The resulting images are presented in Figure 6. As expected, the spectrum of the PI image (Fig. 6d) contains mainly the second-harmonic spectral components. Furthermore, the component at the second-harmonic frequency (7 MHz) highlights a 6-dB higher intensity compared with the initial second-harmonic component, as predicted by Simpson et al. (1999).

Computation time. To provide an idea of the computation times required, the previous cyst simulations have been conducted on the same laptop computer (Intel Core2-Duo T9400 at 2.53 GHz, 3.48 GB of memory) equipped with a nVidia GPU (Quadro NVS 160 M).

The time needed by FieldII to simulate the fundamental image in Figure 3a (linear medium) on the central processing unit (CPU) is assumed as reference. For homogeneous media requiring only one field simulation to compute both fundamental and second-harmonic components, CREANUIS takes between 33 and 38 min to compute the cyst image, compare with the 160 min required by FieldII. For CREANUIS, the exact time depends on the number of discretization points adopted in the GASM simulation.

For a medium with an inhomogeneous coefficient of non-linearity, the GASM simulation is repeated for each RF line according to the corresponding coefficient of non-linearity map. Indeed, the appropriate coefficient of non-linearity $\beta(x, y, z)$ in each point in front of the active elements has to be used to handle the correct variation of the second-harmonic component. In this way, CREANUIS takes between 3 and 10 h using the CPU GASM implementation and between 47 and 87 min using the GPU implementation (Varray et al. 2011a). The computation times are summarized in Table 2.

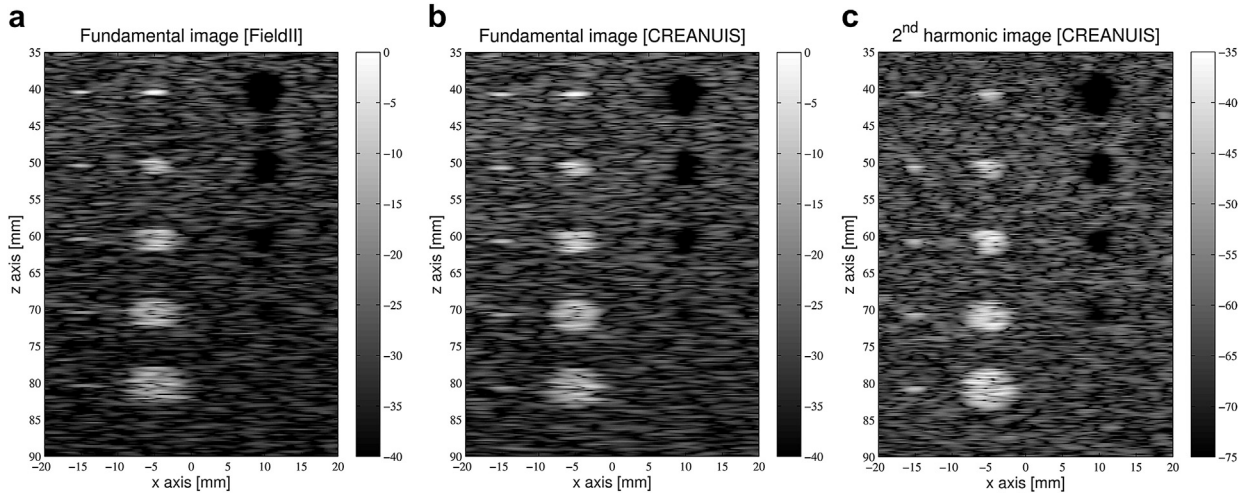

Fig. 4. Image of the cyst phantom including hyper- and hypo-echoic areas of different size. (a) Fundamental FieldII image. (b) Fundamental CREANUIS image. (c) Second-harmonic CREANUIS image.

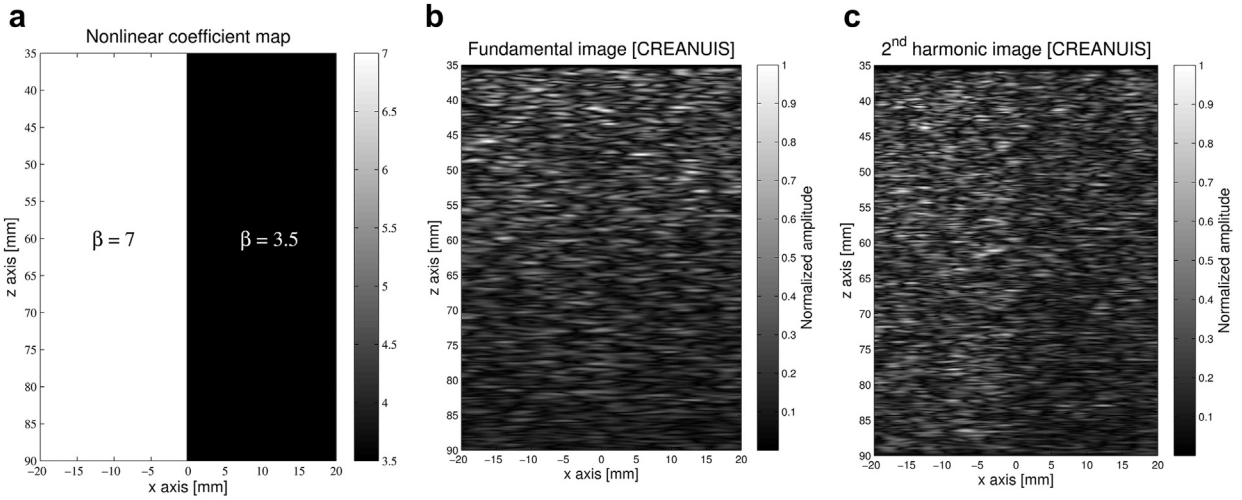

Fig. 5. CREANUIS B-mode images of a medium with an inhomogeneous coefficient of non-linearity. (a) Non-linear map used in generalized angular spectrum method simulations. (b) Fundamental image. (c) Second-harmonic image.

DISCUSSION AND CONCLUSIONS

To our knowledge, no tool has so far combined non-linear ultrasound propagation software and a reconstruction algorithm to create non-linear RF images. With the solution proposed in this article, users can simulate their own beamforming strategy, as typically requested in the design and the optimization of imaging methods based on non-linear propagation. The scatterers' configuration and the image reconstruction are conducted in a similar way as in the FieldII implementation, considering, in particular, the spatial impulse response of the transducer to obtain realistic acoustic images.

The fundamental image provided by CREANUIS has been validated by a comparison with the image based on FieldII. The low mean deviation between the two models (MD = 8.1%) confirms the proximity of the two models. Such a value looks consistent with the previous estimation of the difference between the FieldII and GASM pressure fields, which provided a 2% mean difference and a peak error of 8.5% (Varray et al. 2011b). The images obtained with CREANUIS are closer to the theoretical Rayleigh distribution than those obtained with FieldII. This significantly validates our approach, as the FieldII model is considered as a reference in the US community.

Use of the GASM in CREANUIS provides fast simulations while taking into account media with inhomogeneity in the coefficient of non-linearity. Amplitude modulation, pulse inversion andor other non-linear imaging modalities can be easily and quickly simulated, considering also the possible presence of contrast agents, which have a higher coefficient of non-linearity compared with the surrounding medium (Wu and Tong 1998).

Limitations of CREANUIS have to be mentioned. First, the simulation of microbubble non-linear acoustic response is not currently possible in CREANUIS. The microbubbles have specific characteristics leading to cumulative effects in non-linear imaging: non-linear response, higher coefficient of non-linearity, higher back-scattering amplitude. In CREANUIS, only the coefficient of non-linearity change coupled with arbitrary back-scattering amplitudes is considered. A more complete algorithm would be required to express, for each bubble, the back-scattering amplitude and phase depending on the pressure wave, with a dramatic increase in the computation time.

At present, only the fundamental and second-harmonic components of simulation have been implemented in CREANUIS. This is not a crucial limitation, by considering the limited bandwidth of standard probes and the low amplitude of third and higher harmonics. However, to simulate new non-linear methods such as super-harmonic imaging (Bouakaz et al. 2002), the non-linear propagation simulator can be extended to take into account higher harmonics in the RF data. Another approximation comes from the speed of sound, which is considered constant in the entire medium. This hypothesis is mandatory for the GASM simulation to express the propagation equation in the Fourier domain, and it simplifies the image reconstruction algorithm.

Another limitation concerns the back-scattered signal. Indeed, on the return path, only attenuation is taken into account, whereas non-linear propagation is disregarded. This approximation is justified by the small pressure back-propagated to the probe. A more severe limitation is the fact that only planar sources can be simulated with our GASM implementation. With the current

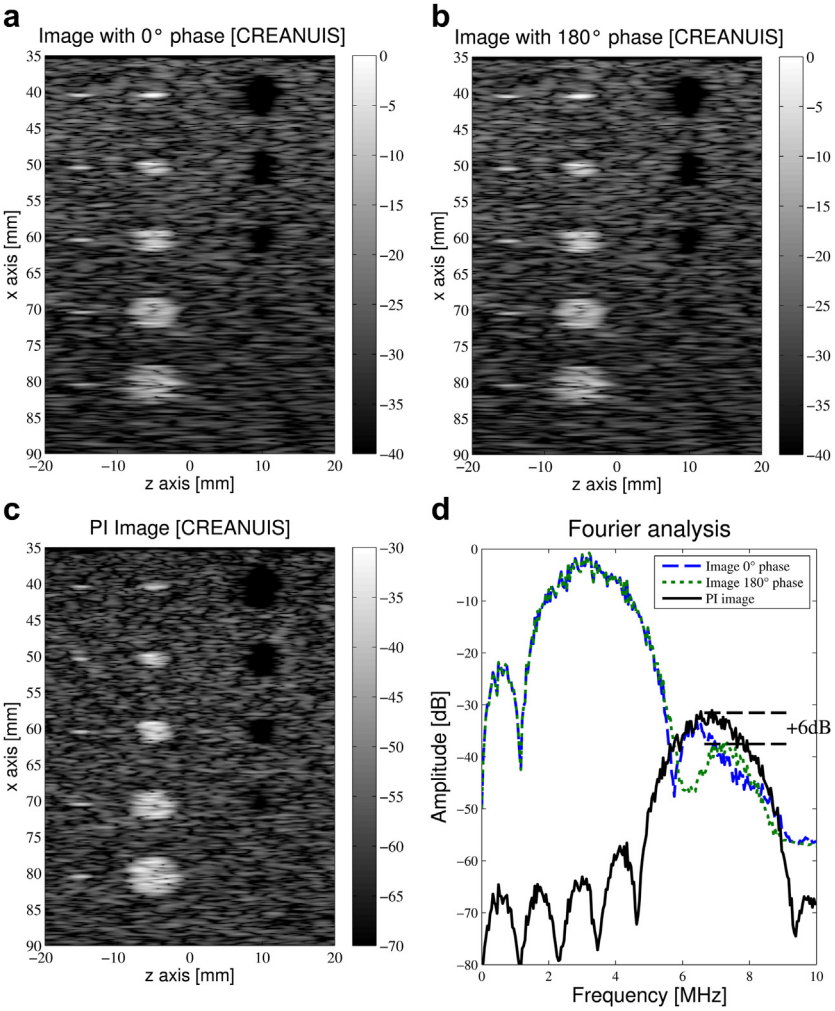

Fig. 6. Pulse inversion (PI) method simulation. (a, b) B-Mode images obtained with 0° and 180° phases, respectively. (c) Pulse inversion image after summation of the first two images. (d) Average Fourier spectrum of the 163 radiofrequency lines in the pulse inversion image.

development of 2-D probes for 3-D imaging, CREANUIS has to be extended to handle more complex situations. Another limitation is the steering of US beams. Currently, steering is available in the GASM part, but not in the image reconstruction. Additional work is required to propose new simulation configurations in CREANUIS. Finally, no bandpass function has been defined on the transducer. Indeed, in transmission, the bandwidth is defined by the signal transmitted in the medium. In reception, an infinite bandwidth is used. If a more realistic transducer effect is required in reception, the final RF image has to be filtered with the desired bandpass filter.

As for FieldII, the CREANUIS computation time strongly depends on the number of scatterers used in the simulation. For media with homogeneous coefficients of non-linearity, only one non-linear field simulation is needed. If a medium with an inhomogeneous coefficient of non-linearity is considered, the non-linear propagation has to be simulated for each RF line, and this substantially increases the total simulation time. Finally, compared

Table 2. B-Mode image computation times obtained with FieldII and CREANUIS

Simulator	Coefficient of non-linearity	Time (min)	Speed-up factor
Field II	Homogeneous	160	1
CREANUIS (GASM on CPU)		[33; 38]	[4.2; 4.8]
CREANUIS (GASM on CPU)	Inhomogeneous	[160; 600]	1
CREANUIS (GASM on GPU)		[47; 87]	[3.4; 6.9]

GASM = generalized angular spectrum method; CPU = central processing unit.

with FieldII simulations, the computation time is decreased by a factor 1.8 to 4.8, depending on whether the coefficient of non-linearity is homogeneous or not. Additional developments are required to further decrease the computation time and to continue to exploit the capabilities of GPUs. Recent works have been proposed to quickly simulate the spatial impulse response of the transducer on a GPU (Shams et al. 2011).

CREANUIS software is free and can be downloaded from the web at http://www.creatis.insa-lyon.fr/site/en/CREANUIS or located by searching for "CREANUIS." The software is the property of CREATIS, INSA-Lyon, Université Lyon 1, CNRS and INSERM.

Acknowledgments—This work was funded by the ANR-11 TecSan-008–01 BBMUT and was supported by the LABEX CeLyA (ANR-10-LABX-0060) of Université de Lyon, within the program "Investissements d'Avenir" (ANR-11-IDEX-0007) operated by the French National Research Agency (ANR). The main author was financially supported by the Franco-Italian University with the Vinci and Galileo Grant and by the Rhône-Alpes region with the Explora'Doc Grant.

REFERENCES

Angelsen B, Hansen R, 2007. SURF imaging: A new method for ultrasound contrast agent imaging. In: Proceedings, 2007 IEEE Ultrasonics Symposium, New York, 28–31 October 2007:531–541.

Averkiou M, Roundhill D, Powers J. 1997. A new imaging technique based on the nonlinear properties of tissues. In: Proceedings, 1997 IEEE Ultrasonics Symposium (Vol. 2), Toronto, 5–8 October, 1997:1561–1566.

Bernard O, D'Hooge J, Friboulet D. Statistics of the radio-frequency signal based on K-distribution with application to echocardiography. IEEE Trans Ultrason Ferroelectr Freq Control 2006;53:1689–1694.

Borsboom J, Bouakaz A, de Jong N. Pulse subtraction time delay imaging method for ultrasound contrast agent detection. IEEE Trans Ultrason Ferroelectr Freq Control 2009;56:1151–1158.

Bouakaz A, De Jong N, Cachard C. Standard properties of ultrasound contrast agents. Ultrasound Med Biol 1998;24:469–472.

Bouakaz A, Frigstad S, Ten Cate FJ, de Jong N. Super harmonic imaging: A new imaging technique for improved contrast detection. Ultrasound Med Biol 2002;28:59–68.

Christopher PT, Parker KJ. New approaches to nonlinear diffractive field propagation. J Acoust Soc Am 1991a;90:488–499.

Christopher PT, Parker KJ. New approaches to the linear propagation of acoustic fields. The J Acoust Soc Am 1991b;90:507–521.

De Jong N. 1993. Acoustic properties of ultrasound contrast agents. Ph.D. thesis, Erasmus University, Rotterdam.

Demi L, van Dongen K, Verweij M. A contrast source method for nonlinear acoustic wave fields in media with spatially inhomogeneous attenuation. J Acoust Soc Am 2011;129:1221–1230.

Didenkulov I, Yoon S, Sutin A, Kim E. Nonlinear Doppler effect and its use for bubble flow velocity measurement. J Acoust Soc Am 1999; 106:2431–2435.

Du Y, Jensen H, Jensen J. Simulation of second harmonic ultrasound fields. In: Proceedings, 2010 IEEE Ultrasonics Symposium, San Diego, CA, 11–14 October 2010:2191–2194.

Du Y, Jensen J. Feasibility of non-linear simulation for field ii using an angular spectrum approach. In: Proceedings, 2008 IEEE Ultrasonics Symposium, Beijing, 2–5 November 2008:1314–1317.

Eckersley RJ, Chin CT, Burns PN. Optimising phase and amplitude modulation schemes for imaging microbubble contrast agents at low acoustic power. Ultrasound Med Biol 2005;31:213–219.

Hallaj IM, Cleveland RO. FDTD simulation of finite-amplitude pressure and temperature fields for biomedical ultrasound. J Acoust Soc Am 1999;105:L7–L12.

Jensen J, Nikolov I. Fast simulation of ultrasound images. In: Proceedings 2000 IEEE Ultrasonics Symposium (Vol. 2), Puerto Rico, 22–25 October 2000:1721–1724.

Jensen JA. Field: A program for simulating ultrasound systems. In: Proceedings, 10th Nordic-Baltic Conference on Biomedical Imaging. Med Biol Eng Comput 1996;34:351–353.

Jensen JA, Munk P. Computer phantoms for simulating ultrasound B-mode and CFM images. In: Lees S, Ferrari LA, (eds). Acoustical imaging, Vol. 23. New York: Plenum Press; 1997. p. 75–80.

Jensen JA, Svendsen NB. Calculation of pressure fields from arbitrarily shaped, apodized, and excited ultrasound transducers. IEEE Trans Ultrason Ferroelectr Freq Control 1992;39:262–267.

Li Y, Zagzebski J. Computer model for harmonic ultrasound imaging. IEEE Trans Ultrason Ferroelectr Freq Control 2000;57:1259–1272.

Mahue V, Mari JM, Eckersley R, Tang MX. Comparison of pulse subtraction Doppler and pulse inversion Doppler. IEEE Trans Ultrason Ferroelectr Freq Control 2011;58:73–81.

Mari JM, Hibbs K, Stride E, Eckersley R, Tang MX. An approximate nonlinear model for time gain compensation of amplitude modulated images of ultrasound contrast agent perfusion. IEEE Trans Ultrason Ferroelectr Freq Control 2010;57:818–829.

Pasovic M, Danilouchkine M, Faez T, van Neer PLMJ, Cachard C, van der Steen AFW, Basset O, de Jong N. Second harmonic inversion for ultrasound contrast harmonic imaging. Phys Med Biol 2011;56: 3163–3180.

Pasovic M, Danilouchkine M, Matte G, van der Steen AFW, Basset O, de Jong N, Cachard C. Broadband reduction of the second harmonic distortion during nonlinear ultrasound wave propagation. Ultrasound Med Biol 2010;36:1568–1580.

Pinton G, Dahl J, Rosenzweig S, Trahey G. A heterogeneous nonlinear attenuating full-wave model of ultrasound. IEEE Trans Ultrason Ferroelectr Freq Control 2009;56:474–488.

Rognin N, Arditi M, Mercier L, Frinking PJA, Schneider M, Perrenoud G, Anaye A, Meuwly J, Tranquart F. Parametric imaging for characterizing focal liver lesions in contrast-enhanced ultrasound. IEEE Trans Ultrason Ferroelectr Freq Control 2010;57: 2503–2511.

Shams R, Luna F, Hartley R. An algorithm for efficient computation of spatial impulse response on the GPU with application in ultrasound simulation. In: Proceedings, 2011 IEEE International Symposium on Biomedical Imaging: From Nano to Macro, Chicago, 30 March–2 April 2011:45–51.

Simpson D, Chin CT, Burns P. Pulse inversion Doppler: A new method for detecting nonlinear echoes from microbubble contrast agents. IEEE Trans Ultrason Ferroelectr Freq Control 1999;46:372–382.

Stepanishen PR. Transient radiation from pistons in an infinite planar baffle. J Acoust Soc Am 1971;49:1629–1638.

Szabo TL. Generalized Fourier transform diffraction theory for parabolically anisotropic media. J Acoust Soc Am 1978;63:28–34.

Tang MX, Eckersley RJ. Nonlinear propagation of ultrasound through microbubble contrast agents and implications for imaging. IEEE Trans Ultrason Ferroelectr Freq Control 2006;53:2406–2415.

Tang MX, Eckersley RJ. Frequency and pressure dependent attenuation and scattering by microbubbles. Ultrasound Med Biol 2007;33: 164–168.

Tang MX, Loughran J, Stride E, Zhang D, Eckersley RJ. Effect of bubble shell nonlinearity on ultrasound nonlinear propagation through microbubble populations. J Acoust Soc Am 2011;129:EL76–EL82.

Treeby BE, Tumen M, Cox B. Time domain simulation of harmonic ultrasound images and beam patterns in 3 D using the k-space pseudospectral method. Med Image Comput Computer-Assisted Interv 2011;6891:363–370.

Van Wijk MC, Thijssen JM. Performance testing of medical ultrasound equipment: Fundamental vs. harmonic mode. Ultrasonics 2002;40: 585–591.

Varray F, Cachard C, Ramalli A, Tortoli P, Basset O. Simulation of ultrasound nonlinear propagation on GPU using a generalized angular spectrum method. EURASIP J Image Video Process 2011a;17:1–6.

Varray F, Ramalli A, Cachard C, Tortoli P, Basset O. Fundamental and second-harmonic ultrasound field computation of inhomogeneous

nonlinear medium with a generalized angular spectrum method. IEEE Trans Ultrason Ferroelectr Freq Control 2011b;58:1366–1376.
Wagner R, Smith S, Sandrik J, Lopez H. Statistics of speckle in ultrasound B-scans. IEEE Trans Sonics Ultrason 1983;30:156–163.
Wu J, Tong J. Measurements of the nonlinearity parameter *B/A* of contrast agents. Ultrasound Med Biol 1998;24:153–159.
Yang X, Cleveland RO. Time domain simulation of nonlinear acoustic beams generated by rectangular pistons with application to harmonic imaging. Journal Acoust Soc Am 2005;117:113–123.
Yu J, Wang Y, Tan J. Simulation of ultrasound harmonic imaging as affected by tissue properties. In: Proceedings, 2011 XXXth URSI General Assembly and Scientific Symposium, Istanbul, 13–20 August 2011:1–4.
Zemp RJ, Tavakkoli J, Cobbold RSC. Modeling of nonlinear ultrasound propagation in tissue from array transducers. J Acoust Soc Am 2003; 113:139–152.
Zhang D, Gong X. Experimental investigation of the acoustic nonlinearity parameter tomography for excised pathological biological tissues. Ultrasound Med Biol 1999;25:593–599.